



HYDRAULIC MODEL EXPERIMENTS  
FOR THE  
DESIGN OF THE BOULDER DAM INTAKE TOWERS

By Joseph Howell Bradley, B.Sc.,  
(University of Illinois, 1929)

A Thesis submitted to the Faculty of the Graduate School of  
the University of Colorado, in partial fulfillment of the require-  
ments for the Degree Master of Science.

Department of Civil Engineering

1937

## TABLE OF CONTENTS

Page

Introduction	
The Intake Towers	
Acknowledgments	
List of Symbols	
The Laboratory and Test Equipment	
The Laboratory	
The Model	
Analysis of Losses in the Intake Tower	
Method of Procedure	
Total Losses Through Tower	
Trash Rack Losses	
Gate Entrance Losses	
Head Required to Change Direction of Flow	
Distribution of Total Discharge Passing Through the Upper and Lower Gate	
Relation of $d_1$ and $D_1$ to the Discharge	
The Upper Arizona Penstock Assembly	
The Model	
Investigation of Pressures at Base of Tower	
Bend Losses	
Penstock Tests	
Intake Tower Electric-Analogy Studies	
Introduction	
The Apparatus	
Tests on a Section of Tower Located Nearest the River	
Tests on a Section of Tower Located Nearest the Canyon Wall	
Summary	
Bibliography	

## LIST OF FIGURES

Figure		Page
1	Boulder Dam Plate Steel Outlet Pipes - General Layout	
2	Intake Tower and Inclined Tunnel	
3	Headers, Penstocks and Conduits in Upper Arizona Tunnel	
4	Laboratory Showing Location of Models	
5	Model of Penstock Assembly - Scale 1:64	
6	Intake Tower Model - Scale 1:64	
7	Model of Arizona Intake Tower Located Nearest the Dam	
8	Miscellaneous Details of Intake Tower	
9	Losses Due to Pure Pipe Friction	
10	Comparison of Piezometer Pressures Below Intake Tower	
11	Total Loss Through Tower with and without Trash Racks	
12	Losses Through Trash Rack	
13	Entrance Losses Through Gates	
14	Head Required to Change Direction of Flow at Gates - Model	
15	Head Required to Change Direction of Flow at Gates - Prototype	
16	Relation of $d_1$ and $d_2$ to the Discharge	
17	Distribution of Flow Between Upper and Lower Gate - Both Gates Open	
18	Relation of $d_1$ to Reynold's Number - Model	
19	Relation of $D_1$ to the Discharge - Prototype	

LIST OF FIGURES (CONTINUED)

Figure	Page
20	Model of Upper Arizona Penstock
21	Relation of Pressure Drops at Piezometers 46, 47, 48 and 49 to the Discharge
22	Minimum Pressures at Base of Intake Tower
23	Loss in Bonds in Upper Arizona Penstock
24	Intake Tower Electric-Analogy Model
25	Electric-Analogy Apparatus Representing a Radial Section of the Intake Tower Located Adjacent to the Canyon Wall
26	Electric-Analogy Results on Radial Section of Tower Nearest the River
27	Electric-Analogy Results on Radial Section of Tower Nearest the River
28	Electric-Analogy Results on Radial Section of Tower Nearest the Canyon Wall
29	Electric-Analogy Results on Radial Section of Tower Nearest the Canyon Wall

UNITED STATES  
DEPARTMENT OF THE INTERIOR  
BUREAU OF RECLAMATION

Branch of Design and Construction  
Engineering and Geological Control  
and Research Division  
Denver, Colorado  
June 1937

Laboratory Report No. 21  
Hydraulic Laboratory  
Compiled by: J. H. Bradley  
Reviewed by: J. E. Warshaw

Subject: Boulder Dam Intake Towers - Thesis

#### INTRODUCTION

The Boulder Dam structures as outlined in the preliminary designs far surpassed any similar structures constructed in the past. Insofar as it was possible, careful laboratory investigations were made concerning the major problems encountered in the design of this dam. One phase of laboratory investigation consisted of testing the major hydraulic features of the dam by means of models. On the whole the models yielded valuable results which aided materially in preparing the final designs for these structures. The major hydraulic features tested by this means were the spillways, the intake towers, the penstocks connecting the intake towers with the turbines and outlet valves, the needle valves in the tunnel plug outlet works, and the future hydraulic conditions in the river downstream from the powerhouse. This thesis constitutes solely a condensation of the laboratory procedure with an analysis of the results obtained from the hydraulic model of one of the Boulder Dam intake towers. A drawing which shows the relationship of the intake structures to the dam has been included as Figure 1.

#### The Intake Towers

The water for irrigation and power purposes will be controlled by the four intake towers adjacent to the upstream face of the

2

Boulder Dam<sup>1</sup>. Each of the intake towers is provided with two cylinder gates 32 feet in diameter; the lower in the base of the tower at elevation 895 and the upper at elevation 1045. (Fig. 2). These gates will serve to control the flow through the 30-foot steel penstock headers that extend from the base of each tower to the turbines in the power plant and to either the canyon-wall outlet works or the tunnel-plug outlet works. The closure of the upper and lower gates in any one intake tower will permit the unwatering of the steel penstock and all its appurtenances for the purpose of inspection and maintenance.

To determine the hydraulic action of these towers and control gates under the various conditions of discharge to which they may be subjected, a model of one of the towers, on a scale of 1 to 64, was constructed and tested in the hydraulic laboratory of the Colorado Agricultural Experiment Station, Fort Collins, Colorado. The model represented the upper Arizona penstock header and manifold assembly with its corresponding intake tower. (Figs. 1, 2, and 3).

These model tests made possible a definite analysis of the losses and flow characteristics in the intake tower; offered a simple yet accurate method of measuring the flow entering the intake towers; and made practical the elimination of a proposed set of air vents at the base of each tower.

#### Acknowledgments

The hydraulic model experiments described in this thesis were performed by the U. S. Bureau of Reclamation in the laboratory of the Colorado Agricultural Experiment Station, Fort Collins, Colorado, under the direction of Jacob E. Warnock, Research Engineer. The author was in charge of the testing of this model. These studies were made under the general supervision of J. L. Savage, Chief Designing Engineer.

---

<sup>1</sup>Hinsie, P. A., Hydraulic Valves and Gates for Boulder Dam, Mechanical Engineering, vol. 56, July 1934, p. 367.

During the experiments a 90-degree V-notch weir was used to measure the water supplied to the model. This weir was calibrated by the Irrigation Division of the U. S. Department of Agriculture and checked by the laboratory staff of the Bureau of Reclamation prior to the testing of the model.

To operate the intake tower model, the two 28-inch diverter gates immediately downstream from the weir (Fig. 4) were closed, thus the water was diverted to the right into a flume which served as a reservoir as well as a supply channel. Adjustable baffles were installed in this flume to eliminate undesirable cross currents produced by the sharp bend at the upstream end. The intake tower model was located in a tank 10-1/2 feet by 10-1/4 feet by 12 feet deep located at the downstream end of this shallow flume.

#### The Model

The model constructed on a scale of 1:24, consisted of a complete assembly of the upper Arizona 30-foot penstock header, intake tower, and branch penstocks leading to the turbines and needle valves (Figs. 5 and 6). Photographs of the model are shown on Figure 7.

The intake tower and the surrounding topography were located as shown in Figures 5 and 7. The inner portion of the tower consisted of galvanized sheet-metal cylindrical shells, accurately built and carefully soldered together with butt joints, forming a true representation of the prototype in detail and dimension. Two independently operated cylinder gates were installed in the tower, similar to those in the prototype. The gates were made of 12-gage seamless steel tubing with the lower outside edges beveled sufficiently to insure a close fit with the base plates forming a satisfactory water seal (Figs. 6-A and 6-B). These were raised and lowered by three small rods attached to each gate at the third points on the circumference. The rods from the lower gate converged into one main rod which extended up the center of the tower to the hoisting apparatus. The upper end of the rod was

A - Intake Tower Without  
Trash Racks

B - Intake Tower with  
Trash Racks

C - Intake Tower Showing Topography  
and Portion of Dam

FIGURE 7 - MODEL OF ARIZONA INTAKE TOWER LOCATED NEAREST  
THE DAM



All engineering work of the Bureau of Reclamation is under the direction of H. P. Valtor, Chief Engineer, and all activities of the Bureau are directed by John C. Page, Commissioner.

The author sincerely appreciates the cooperation of the Bureau of Reclamation in granting him permission to use the material herein as a graduate thesis. The author assumes full responsibility for all statements and conclusions presented, as these are entirely personal and should in no way reflect upon the Bureau of Reclamation.

#### List of Symbols

- $\Delta_1$  Difference in elevation between the water surface outside and inside the tower, foot (model).
- $\Delta_2$  Difference in elevation between the reservoir surface and the reading of piezometer 45 (model).
- $\Delta_3$  Difference in elevation between the reservoir surface and the reading of any one of the five piezometer rings A, B, C, D, and E located below the tower (model).
- $D_1$  Difference in elevation between the water surface outside and inside the tower (prototype).
- $h_t$  Total loss through tower, foot of water.
- $h_{en}$  Entrance loss through upper gate, foot of water.
- $h_{ob}$  Entrance loss through lower gate, foot of water.
- $h_{pa}$  Average head required inside tower to change direction of flow at upper gate (model).
- $h_{pb}$  Average head required inside tower to change direction of flow at lower gate (model).
- $H_p$  Average head required inside tower to change direction of flow at either gate (prototype).
- $h_{f(45-a)}$  Pipe friction from piezometer 45 to bottom of the upper gate (model).

$h_f(C-b)$  Pipe friction from piezometer ring C to the bottom of the lower gate (model).

$h_b$  Compound bend loss in main header directly below intake tower.

$R = \frac{V \cdot D}{\nu}$  "Reynolds" number

$F = \frac{V^2}{g \cdot D}$  Froude's number

$V$  Mean velocity - feet per second.

$D$  Inside diameter of tower - feet.

$g$  Acceleration of gravity - feet per second per second.

$\nu$  Kinematic viscosity  $\frac{\text{ft.}^2}{\text{sec.}}$ , square feet per second.

$\mu$  Absolute viscosity  $\frac{0.0003716}{0.4712 + 0.01435T + 0.0000682T^2}$ ,  
 $\frac{\text{lb. sec.}}{\text{ft.}^2}$ , where  $T$  is the temperature in degrees Fahrenheit.

$\rho$  Density of water at  $T$  degrees Fahrenheit,  $\frac{\text{lb. sec.}^2}{\text{ft.}^4}$

#### THE LABORATORY AND TEST EQUIPMENT

##### The Laboratory

A general layout of the interior of the Fort Collins Laboratory is shown on Figure 4. Water for the experiments was supplied from a reservoir, with a capacity of 30,000 cubic feet, located on a hill adjacent to the laboratory. The flow from the reservoir, controlled by three 12-inch hand-operated gates, passed through a diverging flume into a concrete weir-channel, 19-1/2 feet long, 10 feet wide, and 7-1/4 feet deep. A by-pass gate and a 4-inch by-pass valve were located in one side of the weir channel, 13 feet upstream from the weir. Small adjustments of the discharge passing over the weir were made by varying the flow through these by-passes. The head on the weir was measured by a hook gage and a float gage both operating in a stilling well connected to the weir channel.

threaded to permit raising and lowering the gate by a small crank in the upper part of the tower (Fig. 6-C). The rods to the upper gate were connected in a similar manner to a sleeve which enclosed the main rod leading to the lower gate. This sleeve was also threaded at the upper end, and was actuated by a second crank located in the upper part of the tower.

The bottom portions of the gate entrances were machined metal plates, the lower one forming a base plate as well. The upper portions of the entrances were milled using a mixture of beeswax and paraffin (Figs. 6-A and 6-B). With the exception of the piers and pier spacers, which were of wood, and the gate entrances which were of wax and paraffin, the tower was constructed entirely of metal. The pier and spacer blocks were protected with two coats of aluminum paint to alleviate as much as possible any swelling of these parts of the model. The topography about the tower was constructed from contour maps of the canyon at the dam site, and consisted of a lean mixture of sand concrete. Trash racks (Fig. 7-D) were installed on the tower during a portion of the tests. These were constructed to scale but, due to their miniature size, there is some doubt as to the advisability of relying closely upon the results obtained with them. Small edges and burrs which were practically impossible to remove, surface tension, and traces of grease and oil on the racks all probably had some effect upon the results. The racks (182 feet in length, prototype) were constructed of very thin strips of sheet metal set with the thickness of the metal normal to the direction of flow and held in place by cross pieces to which the strips were soldered. Upon completion of the various parts, the tower was assembled on its base plate and bolted to a corresponding plate located in the floor of the model tank, to which the 30-foot diameter penstock header was connected. In making alterations in the model, it was only necessary to unbolt the upper plate from the lower and remove the intake tower as a unit.

## ANALYSIS OF LOSSES IN THE INTAKE TOWER

### Method of Procedure

To aid in an analysis of the losses in the intake tower, a ring of piezometers was installed in the base at elevation 890.0 (Fig. 6). It was anticipated and later confirmed, that the vertical 90-degree bend in the penstock header immediately below the tower would produce an unbalanced effect upon the flow in this portion of the model, causing a variation in pressure at the four piezometers. As the losses to be measured in the model were small, averaging the readings of this ring of piezometers would have been inaccurate. Furthermore, the velocity distribution in the vicinity of the bend would have been unsymmetrical. To avoid complicating the loss computations with errors from these sources the penstock header was disconnected from the base of the tower model and a straight section of pipe 3 feet in length connected in its place (Fig. 8-A). The lower end of this auxiliary section was fitted with a flange to which orifices of different size were fastened to regulate the discharge through the tower. Five rings of piezometers designated as A to E, inclusive, (Fig. 8-A) were installed at 6-inch intervals along the auxiliary section of pipe. Each ring consisted of four piezometers spaced 90 degrees apart, and each piezometer was connected with a rubber hose to a single glass manometer reading tube. An average value for the pressure at the base of the tower at elevation 890.0 was obtained from these five rings of piezometers by adding the computed pipe friction, from each ring to elevation 890.0 to the corresponding observed gage reading of each.

The section of pipe of which the inner shell of the tower was constructed, and also the auxiliary section temporarily added below, were similar in construction to pipe previously used for other experimental work in the same laboratory. The pipe friction used in these computations was therefore obtained from a previous friction calibration on similarly constructed pipes. A record of the friction calibrations for three sizes of this pipe are included as Figure 9.

Observed pressures at the five piezometer rings below the tower are shown on Figure 10 for several runs with both gates open. Rings A and B are consistent with the other three; ring A appearing to be unaffected by the lower gate, and ring B being uninfluenced by the orifice. The data for each run plotted essentially as a straight line, thus readings from all five rings were used in the loss computations.

Two siphon piezometers were installed in the center of the tower (Fig. 3-A); one midway between the upper and lower gates, and the other about a foot above the upper gate. Each consisted of a piece of 3/16-inch copper tubing drawn to a point at the lower end as shown in Figure 3-B. Twelve 3/64-inch holes were drilled in each tube, perpendicular to the walls, and the two piezometers were suspended vertically in the center of the tower.

One or both gates were always fully open in the tests as they are intended to be so operated on the prototype. These gates are provided for unwatering purposes and not as regulators. The total discharge was measured over the laboratory 90-degree V-notch weir. The magnitude of the discharge that could pass through the tower was regulated by the size of the orifice below the tower and the elevation of the water surface in the model reservoir. The model discharge ranged from 0.15 to 0.90 second-feet which corresponds to approximately 5,000 and 30,000 second-feet, respectively, in the prototype.

#### Total Losses Through Tower

Tests were made to determine the losses through the tower; with and without trash racks for either the upper, the lower, or both gates open; for a range of discharges. For all conditions, the total loss through the tower (Fig. 3-A) was computed using the expression

$$h_t = d_3 - h_f(\Delta-b) - \frac{V^2}{2g}$$

where  $h_t$  = Total loss through the tower to elevation 890.0.

$d_3$  = Difference in elevation between the water surface in the

reservoir and the elevation of the water surface in the manometers connected to piezometer rings A to E, inclusive.

$f_{(A-b)}$  = Pipe friction from elevation 890.0 to piezometers below.

$\frac{v^2}{2g}$  = Velocity head at elevation 890.0.

The pipe friction was computed using the combined observations at the piezometer rings below the tower. The results are plotted logarithmically on Figure 11. The total loss through the tower, expressed in terms of the velocity head in the tower at elevation 890.0, is plotted with respect to Reynolds' number rather than the model discharge; as it is possible to account for differences in temperature in the former and not in the latter. During the tests, the temperature of the water varied from 33 to 50 degrees Fahrenheit. The velocity and diameter of the pipe used to compute Reynolds' number was in all cases that existing in the tower at elevation 890.0.

It was desired to express the model losses with respect to the prototype structure as this was one of the ultimate objectives in performing the model experiments. In the past it has been customary to convert from one to the other by means of Froude's law, but this is not a valid method of conversion when small models are used and viscous effects are appreciable. To perform the transfer by this method it is necessary to assume that the losses, expressed in terms of velocity head, are the same in model and prototype for the same value of Froude's number. With viscous effects present in the model, it can readily be seen that this assumption is not entirely correct.

Reynolds' law, on the other hand, takes into account viscosity in prototype and model but is independent of the force of gravity and consequently centrifugal effects. If the model of the intake tower was exactly similar to the prototype, in dimension and roughness for all heads, and centrifugal effects were exactly similar, it would be

possible to extend the model curves to prototype values of Reynolds' number as shown on Figure 11. This would be a similar procedure to plotting the friction factor,  $f$ , for closed conduits, against Reynolds' number (Fig. 9). In the latter case, all straight circular pipes are similar except for roughness, and Reynolds' number offers the correct model-to-prototype conversion. In the case of the intake tower, however, dissimilar centrifugal effects result in model and prototype so that the Reynolds' number extrapolation is not directly applicable.

Up to the present time, little success has been attained in expressing the relationship of all physical factors in a manner which will permit accurate extrapolation. At the present time, therefore, to correctly interpret prototype losses from models, it is necessary to resort to either of two methods: (1) to build one model large enough to reduce viscous effects to a negligible quantity; or (2) to construct three or more smaller models to different scales. In the first, the transformation could be made directly by Froude's law. In the second, the data from three or more models could be plotted with respect to Reynolds' number. There would result three or more sets of curves (one set for each model) on the graph instead of continuous curves as shown on Figure 11. Each would resemble the set preceding it, but would be flatter and be located lower on the graph. Lines representing similar heads could be drawn through the three or more sets of curves and extrapolated to include the desired prototype range.

As only one small model was used for the intake tower experiments, the model-to-prototype conversion, for lack of a better means, was made for this and the following experiments by the use of Froude's law. Due to the viscous effects in the model, the corresponding actual losses in the prototype will undoubtedly be smaller than those indicated by the following graphs. The actual amount of deviation can be approximated by plotting the data by the two methods shown on

Figure 11 and interpolating between the results. It can be stated with assurance that the actual prototype losses will not exceed those obtained on the model when the conversion is made according to Froude's law.

#### Trash-Rack Losses

The loss in head through the trash racks, for the three gate conditions, is represented by the differences between the three pairs of curves on Figure 11. These differences are plotted separately on Figure 12 showing the trash-rack losses directly for the various conditions of flow.

Only reasonable reliance is assigned to the results of the trash-rack tests. As stated previously, the racks were constructed to scale and exhibited a commendable piece of workmanship; but their miniature size, small imperfections, surface tension, and traces of grease on the racks or oil in the water probably influenced the results. In addition, it was physically impossible to construct the trash-rack bars in the model with a similar degree of roughness to those of the prototype.

Two lengths of trash rack were used in the above tests: (1) a rack 182 feet in length extending continuously over both gates; and (2) two racks 50 feet in length, each of which protected one gate. A detailed inspection of the points from which the lines were drawn on Figure 11 shows that the total losses through the tower for the two lengths of trash rack were quite analogous for the same conditions of flow, which indicates that above a certain length, factors other than the length of the racks determine the losses through them.

During the tests, the only place where trash collected on the racks was directly in front of the gates; the remainder of the racks were continuously clean. Trash racks are further discussed in this thesis under the heading, "Intake Tower Electric-Analogy Studies."



### Gate Entrance Losses

The entrance loss through the upper gate is the difference between the energy head at the water surface of the reservoir and at the bottom of the upper gate. The trash racks were removed before the individual losses in the gate tower were measured.

The entrance loss through the upper gate (Fig. 3-D) was computed using the equation.

$$h_{ca} = d_2 - h_f(45-a) - \frac{v^2}{2g}$$

where  $h_{ca}$  = Entrance loss through the upper gate.

$d_2$  = Difference in elevation between the water surface in the reservoir and the water surface in piezometer 45.

$h_f(45-a)$  = Pipe friction from piezometer 45 to the bottom of the upper gate.

$\frac{v^2}{2g}$  = Velocity head at piezometer 45.

The entrance loss through the lower gate is the difference between the energy head at the water surface of the reservoir and at the bottom of the lower gate. This loss (Fig. 3-D) was computed using the equation:

$$h_{ob} = d_3 - h_f(A-b) - \frac{v^2}{2g}$$

where  $h_{ob}$  = Entrance loss through the lower gate.

$d_3$  = Difference in elevation between the water surface in the reservoir and the water surfaces in piezometer rings A to E, inclusive.

$h_f(A-b)$  = Pipe friction from elevation 890.0 to the piezometers below.

$\frac{v^2}{2g}$  = Velocity head computed at elevation 890.0.

The curves on Figure 13 show the entrance losses computed for these two conditions of flow. The losses are expressed in terms of the velocity head computed in the tower at elevation 890.0, and are plotted

with respect to Reynolds' number for the model, computed at the same point. An additional scale has been superimposed on this graph so that the entrance losses can also be expressed in terms of the prototype discharge, computed according to Froude's law. The entrance conditions to the lower gate are slightly superior to those at the upper gate. It is evident from the preceding explanation that the entrance loss curve for the lower gate, shown on Figure 13 is the same as that for the total loss curve, without trash racks, shown on Figure 11; as the entrance loss is the total loss in this case. In the case of the upper gate, the entrance loss is smaller than the total loss through the tower as it is necessary to deduct pipe friction.

The sources of error exist in this analysis:

1. The mean velocity head has been used in the computations as it was impractical to measure the velocity distribution in the tower to obtain the true energy head for each condition of flow. The velocity distribution in the tower is undoubtedly of a complex nature.

2. Where it was necessary to compute the surface friction in the tower or in the auxiliary section of pipe below the tower, reference was made to the curves on Figure 9. The pipes from which these curves were obtained were similar to the inner portion of the tower and any error that might arise from this source is small; as in no case did the length of pipe considered in the friction computations exceed 2.5 feet or 5.3 diameters. It is well to again mention that the prototype losses as shown on the graphs are only approximate.

#### Head Required to Change Direction of Flow

As the water enters the gates in nearly a horizontal direction, a definite force is required to produce a vertical acceleration. By measuring the pressures directly above and below each gate, it was possible to compute the magnitude of the force acting within the tower.

It was originally intended to obtain the hydraulic losses in the tower by observing the difference in elevation of the water surface outside and within the tower. The existence of this force, however, produced a rise in the surface level in the tower and made the proposed method of computation impractical.

The head required to change the direction of flow at the upper gate (Fig. 6-D), with the lower gate closed, was found experimentally by the following equation:

$$h_{pa} = d_2 - d_1 - h_f(45-a)$$

where

$h_{pa}$  = Hydrostatic head in feet of water required to change the direction of flow at the upper gate.

$d_2$  = Difference in elevation between the water surface in the reservoir and the water surface in piezometer 45.

$d_1$  = Difference in elevation between the water surface in the reservoir and the water surface in the tower.

$h_f(45-a)$  = Pipe friction from piezometer 45 to the bottom of the upper gate.

The head required to change the direction of the flow at the lower gate (Fig. 8-D), with the upper gate closed, was computed in a similar manner, using the equation:

$$h_{pb} = d_3 - d_1 - h_f(A-b)$$

where

$h_{pb}$  = Hydrostatic head in feet of water required to change the direction of flow at the lower gate.

$d_3$  = Difference in elevation between the water surface in the reservoir and the water surface in piezometer rings A to E, inclusive.

$d_1$  = Difference in elevation between the water surface in the reservoir and the water surface in the tower.

$h_f(A-b)$  = Pipe friction from elevation 890.0 to the piezometers below.

The head required to change the direction of flow at the upper and the lower gate, expressed in terms of the velocity head, is plotted with respect to Reynolds' number for the model on Figure 14.

A consideration of the principles of impulse and momentum provides a means of deriving theoretically the force required to change the direction of flow at the gates. It is not possible to obtain a rational theoretical solution from the forces acting entirely within the tower as the conditions of flow at the gates are too indefinite. Another logical method of attack is available, however, which is based on experimental data.

A free jet of water directed against a flat plate exerts a total force on the plate in the direction of the main jet equal to that given by the following expression:

$$F = wA \frac{v^2}{g}$$

where

$F$  = Total Force exerted on plate.

$w$  = Unit weight of water.

$A$  = Area of main jet.

$v$  = Velocity measured in jet.

$g$  = Acceleration of gravity.

By analogy, if the direction of flow is reversed and water is assumed to flow radially inward toward the center of a circular plate and then turn downward away from the plate to form a solid column as in the case of the intake tower, the same law is assumed to apply. Professor A. H. Gibson<sup>2</sup> shows the bulb of pressure developed on a flat plate. The analogy with the intake tower is illustrated on Figure 8-B. If it were possible to measure the pressure at a number of points within the tower, at one of the gates, the pressure distribution might very easily resemble that shown on Figure 8-B. From experiments by Gibson, it seems reasonable to assume that the maximum pressure head is the center of

---

<sup>2</sup>Gibson, A. H. Hydraulics and its Applications, pp. 368 and 371.

the tower is practically the velocity head, while the pressure at the inside face of the tower is approximately 0.66 of the velocity head. By integrating the pressures acting on individual small areas within the tower, an average pressure head of 0.82 of the velocity head is obtained. This is the average height at which the water must stand within the tower to deflect the entering jets to a direction vertically downward.

The component in any direction of the total change in momentum between two points per unit time is the component of force in that direction required to produce this change. If the velocity of the water at the edges of the pressure bulb, outside of the tower, is assumed to be in a horizontal direction, the vertical component of the momentum at this point is zero. The change of momentum per unit time, or the total force in the vertical direction required to produce the change between this point outside the tower and a point within the tower, in the vertical jet below the intake is

$$F = wA \frac{v^2}{g}$$

This expression is identical with that for the total pressure on a flat plate.

If the pressure distribution required to produce the total force,  $F$ , is assumed to be similar to that of the flat plate, then the maximum pressure head is  $\frac{v^2}{2g}$  and the distribution is as shown in Figure 8-E.

With this distribution, the average pressure head within the tower should be:

$$h_p = 0.82 \frac{v^2}{2g}$$

The theoretical values have been plotted on Figure 14 together with the actual values obtained on the model. The agreement is reasonably close and indicates that the analysis is a logical one. From the point of view of structural design, it is of interest that substantial upward reactions exist in the converging intake passages which under

some circumstances might require structural provisions in the design.

To display the information obtained on the model in a more practical form, the model results were transferred into prototype values according to Froude's law and plotted on Figure 15. In this case, the average head of water required inside the tower to change the direction of flow of the water entering is plotted against the prototype discharge. These curves apply only for the upper and lower gate, operating separately.

#### Distribution of Total Discharge Passing Through the Upper and Lower Gate.

It was desired to determine what portion of the total discharge passed through each gate when both gates were fully open. The piezometric drop,  $d_2$ , (Fig. 8-D) bears a definite relationship to the discharge passing through the upper gate; the piezometric drop,  $d_1$ , also shows a relationship to the discharge through the upper gate; and the two sets of data, when plotted logarithmically with respect to the model discharge, result in two straight lines (Fig. 16).

Using these relationships, it was possible to compute the discharge through the upper gate when both gates were in operation. In other words, the pressure drops,  $d_1$  and  $d_2$ , continued to be proportional to the discharge through the upper gate when both gates were in operation. These values were much smaller when both gates were open however, as in this case practically the same total discharge was divided between two gates. For runs in which both gates were operating, the discharge through the upper gate was read from Figure 16 for values of both  $d_1$  and  $d_2$ , and the two discharges averaged for each run. The average was considered the discharge through the upper gate, while the remainder of the total discharge flowed through the lower gate. Figure 17 shows the percentage of the total discharge flowing through each gate. The distribution of flow is expressed with respect to Reynolds' number, computed for the total flow at elevation 890.0 for the model; and a second scale above the graph shows the approximate distribution with respect to the

total prototype discharge. Figure 17 indicates that the flow through the upper gate will be approximately 40 percent of the total regardless of the lake elevation and magnitude of the discharge, providing the lake elevation remains above the upper gate.

#### Relation of $d_1$ and $D_1$ to the Discharge

As the difference in elevation of the water surface outside and within the tower,  $d_1$ , is proportional to the discharge, this relationship may have a practical value. Values of  $d_1$  have been plotted with respect to Reynolds' number, computed at elevation 590.0 for the model with the upper, the lower, or both gates open, on Figure 18. The drop,  $d_1$ , is the same for a given discharge with either the upper or the lower gate operating.

Although the drop,  $d_1$ , (Fig. 3-D) consists of the gate entrance loss plus a small portion of the velocity head, it is a linear measurement; and by Froude's law was converted into an approximate prototype value by multiplying it by the model scale. This drop,  $d_1$ , will be designated by the symbol,  $D_1$ , when converted to the prototype. Values of  $D_1$  are plotted with respect to the prototype discharge on Figure 19. This relation may prove useful for measuring the discharge through the prototype intake towers. The value of  $D_1$  could be obtained by installing two float gages, one on the outside and one on the inside of each tower. Entering the curves on Figure 19 with these values, the approximate discharge flowing through the towers could be obtained.

The relation of  $D_1$  to the discharge has been plotted on Figure 19 for both conditions, with and without the trash racks in place. It is felt that the curves shown for the condition, without the racks, are essentially correct. It has been previously stated that the friction loss through the model trash racks was undoubtedly excessive; therefore, it can quite definitely be stated that the curves on Figure

19, for the model trash racks installed, are higher than would be similar curves made from actual results on the prototype.

It will be possible to actually calibrate the prototype intake towers by the Gibson Method<sup>3</sup> at the time that the acceptance tests are made on the turbines. With the information available on Figure 19 only a few points would be necessary to establish a true calibration curve for the prototype.

#### THE UPPER ARIZONA PENSTOCK ASSEMBLY

##### The Model

At the conclusion of the tests on the intake tower, the 3-foot vertical section of straight pipe below the tower was removed, and the penstock assembly model, constructed on a scale of 1:64, connected in its place (Fig. 5). The assembly consisted of accurate, butt-jointed, smooth sheet-metal pipe. The bends, a 90-degree, 5-5/8-inch diameter vertical bend directly below the tower and a 40-degree horizontal bend of the same diameter located a short distance downstream, were molded of transparent pyralin. The four turbine penstocks (Figs. 3, 5, and 20), 2-7/16 inches in diameter, were connected to the penstock header

#### FIGURE 20 - MODEL OF UPPER ARIZONA PENSTOCK

at a developed angle of 105 degrees in a downstream direction as shown.

<sup>3</sup>Gibson, Herman R., Pressure in Penstocks Caused by the Gradual Closing of Turbine Gates, Trans. Am. Soc. of Civil Engineers, vol. LXXIII, p. 707.



The six 1-19/32-inch diameter branches leading to the canyon-wall outlets were connected to the downstream end of the penstock header by a reduction manifold.

The discharge through the four turbine branches was controlled and measured by sharp-edged circular orifices with diameters of either 0.75 or 0.875 inches. The flow through the six needle-valve branches was controlled and measured in a like manner by orifices with diameters of either 1.006 or 1.250 inches. The head on each orifice was observed from a piezometer located in the end of each branch. These orifices were previously calibrated in similar positions by weighing the discharge.

Piezometers for measuring the pressure intensities were installed in rings at intervals down the main header (Fig. 5). A ring consisted of four piezometers spaced 90 degrees apart, and each piezometer was connected to an individual reading glass on the manometer board.

#### Investigation of Pressures at Base of Tower

In the original design of the intake towers, air vents were provided in the region below the lower gate to relieve any negative pressures which might be created by the conditions of flow. A question arose as to the necessity of these vents and piezometers 46 to 49, inclusive, (Figs. 6, 21-D and 21-E) were installed to study the pressure conditions at this point.

Tests were made with the upper, the lower, and both gates open, and the piezometric drops,  $d$ , between the water surface in the reservoir and the water surfaces in the four piezometers, were recorded. These drops, converted into prototype values, are plotted against the discharge for the individual piezometers for the three conditions of gate opening on Figure 21. For the upper gate open and lower gate closed, (Fig. 21) the drop,  $d$ , recorded at piezometer 46 consists of the following:

$$d = K_f(b-u) + \frac{V^2}{2g} + h_{cu} + h_p$$

where

$d$  = Difference in elevation between the water surface in the reservoir and the water surface in piezometer 46.

$h_{f(b-u)}$  = Pipe friction from piezometer to bottom of upper gate.

$\frac{v^2}{2g}$  = Velocity head at piezometer 46.

$h_{eu}$  = Entrance loss at upper gate.

$h_g$  = Drop in pressure at the piezometer caused by irregularity of flow and suction effect.

The largest piezometric drop occurs at piezometer 46 for all conditions of flow. The curves for piezometer 46 (Fig. 21) were replotted on Figure 22 for the three conditions of gate opening. In addition, two other curves have been superimposed on this graph, which indicate the maximum approximate discharge that can be obtained with all needle valves operating and with all needle valves and turbines operating for various levels of the reservoir. From these two sets of curves, the pressure at piezometer 46 may be obtained for any particular discharge. For example, with the water surface in the reservoir at elevation 1200 and a discharge of approximately 21,000 second-feet through the lower gate (Fig. 22), the water surface in piezometer 46, expressed in prototype, would stand at 42 feet below the reservoir water surface, or elevation 1158, and a pressure of 268 feet of water would exist at the point where this piezometer is located. For the same discharge passing through the upper gate, the water surface in piezometer 46 would stand at elevation 1170. For a discharge of 21,000 second-feet flowing through both gates, the water surface in piezometer 46 would stand at elevation 1174. The water surfaces in the other three piezometers would stand above this elevation. From these results it is evident that a vacuum cannot exist at the base of the tower and air vents are unnecessary.

### Bend Losses

The combined loss for the two bends directly below the tower (a 90-degree vertical bend and a 40-degree horizontal bend interconnected by a straight section 0.88 diameters long, Fig. 3), was obtained from runs in which only the upper gate was open. Flow through the lower gate would have materially affected the velocity distribution in the bends. The loss was obtained by the equation:

$$h_b = d_x - \left\{ \frac{v^2}{2g} + h_f + h_t \right\}$$

where

$h_b$  = Combined bend loss.

$d_x$  = Difference in elevation between the water surface in the reservoir and the average water surface in the manometer tubes connected to piezometers 9 to 12, inclusive (Fig. 5).

$\frac{v^2}{2g}$  = Velocity head at base of tower (elevation 890.0).

$h_f$  = Pipe friction from piezometers 9, 10, 11, and 12 to the downstream edge of the horizontal bend.

$h_t$  = Total loss in intake tower.

A better velocity distribution existed at piezometers 9 to 12 than at 5 to 8 so the former were used in the computations.

The combined loss for the two bends expressed in terms of the velocity head at the base of the tower is plotted with respect to Reynolds' number for the model on Figure 23. An additional scale has been superimposed on the upper portion of the graph from which the approximate bend loss for the prototype can be obtained.

### Penstock Tests

Tests were made on the complete penstock assembly (Figs. 5 and 20) during which the individual discharges, heads, pressures, and flow combinations were recorded. This resulted in a voluminous amount of

data pertaining to the unlimited combinations of flow through the six needle valves and four turbines. With variations in the head, discharge, discharge combinations, and in the sizes of the needle valve and turbine orifices, the variables became so numerous that it was impossible to express the results in a condensed form despite an attempt to record the material in a limited amount of space in this thesis. This information however is on record for immediate reference in the laboratory files.

## INTAKE TOWER ELECTRIC-ANALOGY STUDIES

### Introduction

The electric-analogy method, previously used in the analysis of problems of seepage through earth dams and under masonry dams on porous foundations<sup>4</sup>, was applied as a means of determining the direction of flow of water entering the intake tower. It was anticipated that this would offer a simplified means of determining trash rack areas and incidentally it was desired to study the merits of the method itself. It is a known fact that this method is limited but within limits it has promising possibilities.

### The Apparatus

The apparatus consisted of a shallow glass tray 39 inches long, 18 inches wide, and 3 inches deep equipped with a leveling screw at each corner. A radial section of the tower constructed of redwood, on a scale of 1:100, was cemented to the bottom of the tray. Copper plate electrodes were placed in position in the tray and a solution of sodium chloride used as a conductor. A drawing of the apparatus is shown on Figure 24, and a photograph of the tray in a vertical position is shown on Figure 25. The current used in the experiments was obtained from a 110-volt, 60-cycle source. By inserting a bank of lamps in series with the apparatus as shown on Figure 24, the potential across the electrodes was reduced to about 20 volts. A high-resistance wire, one meter in length stretched on a meter stick on one side of the tray, was connected in parallel with the circuit to constitute a Wheatstone bridge. A spring was attached to one end of this wire to keep it taut at all times as the current raised the temperature of the wire and lengthened it. A metal terminal on one end of the meter stick made a continuous contact with the stretched wire keeping the length connected in the circuit at exactly one meter,

---

<sup>4</sup>Lane, E. W., Campbell, F. B., and Price, W. H., The Flow Net and the Electric Analogy, Civil Engineering, October 1934, and U.S.B.R. Technical Memorandum No. 388.

FIGURE 25 - ELECTRIC-ANALOGY APPARATUS REPRESENTING A RADIAL SECTION OF THE INTAKE TOWER LOCATED ADJACENT TO THE CANYON WALL.

regardless of expansion or contraction. A circuit was established from a sliding contact on the high-resistance wire to the liquid conductor by a wire which had connected in series with it a set of headphones and a probing pencil. All connections in the apparatus were made with heavy copper wire of very low resistance.

The radial section of the tower was represented by setting the tray on a slope with the electrolyte at some depth on the center-line of the tower, as shown in Section A-A, Figure 24. The variables in the experiment were the length of the trash racks, the three gate combinations, and the positions of the electrodes. The apparatus in Figure 24 represents a section of the tower nearest the river with both gates open. The long electrode was connected to one side of the circuit and the two small electrodes in the tower were connected to the other side. The lines resembling contours represent points of equal potential. The purpose of the apparatus was to determine the position of these lines for different percentages of the total potential drop across the electrodes.

The position of any particular potential line was determined by setting the sliding contact on the resistance wire at the point giving the desired potential drop, and moving the probing pencil about in the salt solution until a point was reached at which the absence of a hum in the headphones indicated that no current was flowing through them. To find the position of the potential line representing two percent of the drop between electrodes, the sliding contact would be set at a point on the resistance wire representing two percent of its length, or two centimeters on the meter stick, and the probing pencil moved about in the electrolyte until the alternating-current hum in the headphones faded. This indicated that the probing pencil was at a point in the solution where the potential drop was two percent of the total drop across electrodes. Other points would be located in a similar way with the same setting of the sliding contact until the number was

sufficient to draw the two-percent line. Other potential lines would be located in a similar manner.

#### Tests on a Section of Tower Located Nearest the River

The first tests were made on a radial section of the tower located nearest the river with the electrodes in the positions shown in Figure 24. These tests were made with three different lengths of trash rack; 306 feet, 182 feet, and two 50-foot racks. The resulting equipotential lines are shown on Figures 26 and 27.

Comparing tests 2 and 6, (Figs. 26 and 27) in which the upper gate was closed and the trash-rack lengths were 50 feet and 306 feet, respectively, the corresponding equipotential lines practically coincide, which indicates that the total potential drops between electrodes agree closely. This means that the resistance to flow through the 50-foot rack was no greater than that through the 306-foot rack.

Tests 1 and 5 (Figs. 26 and 27) were made under the same conditions except that the lower gate was closed and the upper gate open. Again the potential lines show a very close agreement, which indicates that the loss was no greater through the 50-foot rack than through the 306-foot rack.

Tests 3 and 4 (Fig. 26) were made on the same segment of the tower with both gates open. The potential lines with the two 50-foot racks agree very well with those for the 306-foot rack. The agreement of the potential lines is not as close for the range from one percent to five percent as the points for these lines were more difficult to locate than those for the larger potential drops. The experiments thus far indicate that, with the racks free from trash, a length of 50 feet in front of each gate will provide sufficient rack area on the river side of the tower.

Tests 7 and 8 (Fig. 27) were made on the same radial section of the tower with a 182-foot trash rack as in the final design. These



however, cannot be directly compared with the tests previously described as the positions of the electrodes were shifted and the tilt of the tray changed. They are included as a matter of record.

#### Tests on a Section of Tower Located Nearest the Canyon Wall

A similar set of tests (Figs. 28 and 29) was made on a radial section of the tower located on the side nearest the canyon wall (Fig. 25). Tests 11 and 14 (Figs. 28 and 29), made with the upper gate closed using two 50-foot and one 306-foot rack, respectively, show a difference in the positions of the potential lines. This indicates that the total potential drop across the electrodes for the 50-foot racks was greater than that for the 306-foot rack. The increase is due to the new boundary conditions which reduce the area of approach and change the direction of the flow to the gates. With this decrease in approach area there must be an increase of velocity to maintain continuity of flow. As velocity is proportional to potential gradient, the gradient must increase as the trash racks and gate openings are approached. This increase is indicated by a reduction in the distance between equipotential lines. Closely spaced potential lines indicate flow concentrations and likewise high velocities.

Tests 10 and 13 (Figs. 28 and 29) were made with the upper gate open and the lower gate closed using two 50-foot racks and one 306-foot rack, respectively. A noticeable increase in the resistivity of the circuit was again witnessed when the 306-foot rack was replaced by the two 50-foot racks.

Tests 9 and 15 (Figs. 28 and 29) were made with both gates open using two 50-foot racks and one 306-foot rack, respectively. There was little difference in the positions of the potential lines from the two assumptions. This could logically be expected as the same discharge was divided between the two gates, and the effective rack area was doubled in the case of the two 50-foot racks. With one gate open, flow could occur only through one 50-foot rack.

Tests 12 and 16 (Figs. 28 and 29) represent flow through the upper and lower gate, respectively, with 182-foot trash racks as finally designed. These results, however, cannot be directly compared with the others as the tilt of the tray was changed and the positions of the electrodes shifted.

The losses shown by the second set of experiments are exceptionally high as flow conditions were not truly represented. In the experiment, all water was assumed to flow downward on the canyon-wall side of the tower, while actually a large portion will flow around the tower as well.

Flow nets have been drawn for tests 7, 10, and 15 (Figs. 27, 28, and 29). According to hydrodynamics, the flow lines should cross the potential lines at right angles. The volumes bounded by the flow lines may be considered as stream tubes, each carrying an equal quantity of water. To establish one end of each flow line, it was assumed that the velocity was constant across the electrode sections inside the tower. The electrodes were then divided into segments which, if revolved, would form annular rings. From these the flow lines were projected and drawn perpendicular to the equipotential lines.

In the two-dimensional flow net where the electrolyte is constant in depth, the dimensions of a rectangle formed by the net bears a constant ratio to every other rectangle in the net by which the average velocity in each stream tube can be determined. For flow nets drawn for tests 7, 10, and 15 (Figs. 27, 28, and 29) this ratio does not exist. With a sloping tray, the flow net is altered by a third dimension. The stream tubes in the three-dimensional net have no parallel sides and it is not possible to obtain the velocities directly from the length or breadth of the rectangles as in the two-dimensional system. The purpose in drawing the flow lines in tests 7, 10, and 15 was merely to indicate the direction of flow. It is possible, however, to obtain the velocities in these three-dimensional nets by a simple but laborious method.

There are eight stream tubes in test 7 (Fig. 27), each carrying

an equal quantity of water. The discharge through each tube is equal to one-eighth of the total discharge flowing into this radial segment of the tower. Figure 3-7 shows a portion of a stream tube in a two-dimensional net, and Figure 3-8, a portion of a stream tube in a three-dimensional net. In the first,  $d$  is a constant throughout, while in the second it is a variable. The velocity at any point in either stream tube is  $V = \frac{q}{wd}$ , where  $q$  is the discharge through the stream tube.

If the velocity is known at any point in the two-dimensional net, it is only necessary to measure  $w$  to obtain the velocity at any other point. In the three-dimensional net,  $d$ , a variable but known at all points, must also be considered in computing the velocities.

The greatest source of error in obtaining velocities in a three-dimensional flow net of this type is not in the computations but in the construction of the net. It is usually necessary to make one or two assumptions before attempting to draw a net, and after these are made and the net commenced, it is still necessary to use a certain amount of judgment as the potential lines are the only definite guides.

There are seven stream tubes entering the upper gate and eight entering the lower, each carrying an equal discharge. This would indicate that 47 percent of the flow was passing through the upper gate and 53 percent through the lower. On the opposite side of the tower where the area of approach is not restricted, the proportion of the total flow through the upper gate should be less, with the result that a greater percentage of the total flow should pass through the lower gate. To obtain the correct proportion of flow through the upper gate, the electrodes in the tower were shifted by trial until the indicated flow through each gate agreed with that measured on the hydraulic model. The above results show that the electric-analogy method is applicable for this type of problem, especially where only one intake is involved, as information can be obtained both readily and at little expense regarding trash-rack areas and obstructions to flow. The double intake on the Boulder Dam gate towers complicated the problem considerably.

## SUMMARY

It is felt that the method employed in analyzing the model results on the intake tower and penstock assembly was sufficiently accurate and the results dependable insofar as the model data is concerned. It was desired, however, to extrapolate the model results to apply for prototype values as this was one of the objects in performing the experiments. With a single small model of this type it is not possible to accurately interpret the conditions that will prevail on the prototype.

The extrapolation from model to prototype has in the foregoing graphs been made according to Froude's law for lack of a more accurate and definite method. As a result, the losses, as plotted with respect to the prototype discharge, are unquestionably larger than those that will actually exist on the prototype. It is predicted that the losses in the full-size structure will probably range from 5 to 20 percent less than those indicated by the graphs. For this reason, it is advisable to refer to the prototype values, as shown on the graphs, not as absolute but approximate values.

From this and previous electric-analogy studies it is apparent that this method can be adapted to many flow problems. Although calculations by this method are usually far from final such solutions make it possible to foresee advantages and disadvantages in a structure far in advance of the final design. The outstanding advantages in using the electric-analogy method, where applicable, are its simplicity, its speed in obtaining results, and its low cost. It is important, however, in interpreting the results of a study of this nature to keep in mind the limitations of the method. The symmetry and precision of the results are a temptation to extend the method at the expense of factors which cannot be considered in the apparatus.

## BIBLIOGRAPHY

- AEGUS, R. W., Intakes for Power Plants, Bulletin No. 6, Section 11, University of Toronto, Faculty of Applied Science and Engineering, School of Engineering Research, 1926.
- BALCH, Leland E., Investigation of Flow through Four-Inch Submerged Orifices and Tubes, Engineering Series, Vol. 3, No. 3, Engineering Experiment Station, University of Washington, Seattle.
- BLAISSELL, P. W., Comparison of Sluice-Gate Discharge in Model and Prototype, Proc. A.S.C.E., January 1936, p. 65.
- CHICK, Alton C., Dimensional Analysis and the Principle of Similitude as Applied to Hydraulic Experiments with Models, Hydraulic Laboratory Practice, A.S.M.E., 1929, pp. 775-827.
- GIBSON, A. H., Hydraulics and its Applications, pp. 192-215, 136-146, 368-371.
- GIBSON, Norman R., Pressures in Penstocks caused by the Gradual Closing of Turbine Gates, Trans. A.S.C.E., Vol. LXXXIII, p. 707.
- GROAT, B. F., Theory of Similarity and Models, Trans. A.S.C.E., Vol. 96, 1932, pp. 273-387.
- HAMILTON, James B., Suppression of Pipe Intake Losses by Various Degrees of Rounding, Bulletin No. 57, Engineering Experiment Station, University of Washington, Seattle.
- HARRIS, Chas. W., The Influence of Pipe Thickness on Re-Entrant Intake Losses, Bulletin No. 48, 1928, Engineering Experiment Station, University of Washington, Seattle.
- HARRIS, Chas. W., Elimination of Hydraulic Eddy Current Loss at Intake, Agreement of Theory and Experiment, Bulletin No. 54, Engineering Experiment Station, University of Washington, Seattle.
- HODGSON, J. L., The Laws of Similarity for Orifice and Nozzle Flow, A.S.M.E., Vol. 50, 1928, APM 50-3.
- HOSIG, I. B., The Deflection of a Free Fluid Jet by a Flat Plate, U.S.E.R. Technical Memorandum No. 541. (Translation from German).
- KINZIE, P. A., Hydraulic Valves and Gates for Boulder Dam, Mechanical Engineering, Vol. 56, July 1934, p. 387.
- KUNZ, Jakob, Jets from Manifold Tubes, Transactions A.S.M.E., APM 53-14, pp. 181-186.

PIGOTT, R. J. S., The Flow of Fluids in Closed Conduits, Transactions  
A.S.M.E., August 1933, pp. 497-515.

ROGERS, T. C., and SMITH, T. L., Experiments with Submerged Orifices  
and Tubes, Eng. News, Nov. 2, 1916.

SEELEY, Fred B., The Effect of Mouthpieces on the Flow of Water through  
a Submerged Short Tube, Bulletin No. 96, Engineering Experiment Station,  
University of Illinois.

SMITH, J. F. D., Calibration of Rounded-Approach Orifices, Trans.  
A.S.M.E., Vol. 56, 1934, RP 56-10, p. 791.

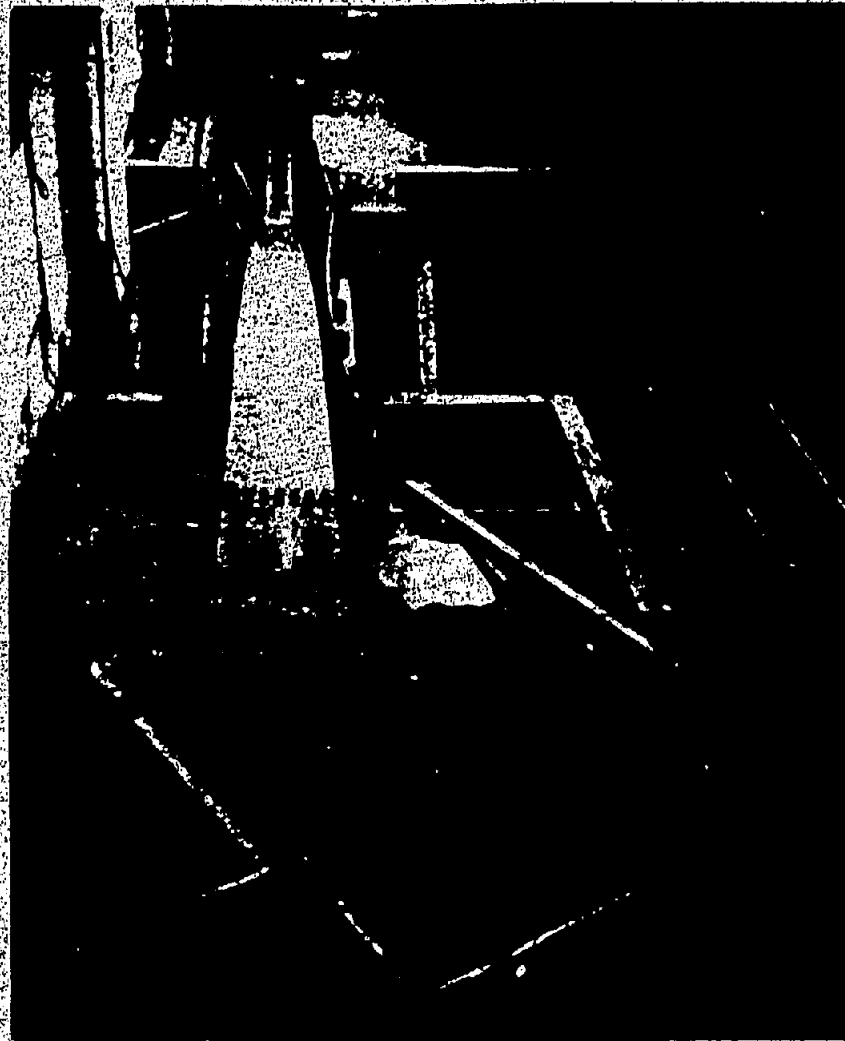
SPITZGLASS, J. M., Similarity Limitations and its Application to  
Fluid Flow, Trans. A.S.M.E., HYD 52-7C, pp. 111-121.

STEWART, C. B., Investigation of Flow through Large Submerged Orifices  
and Tubes, University of Wisconsin, Bulletin No. 216.

THOMA, Prof. D., Hydraulic Losses in Pipe Fittings, U.S.B.R. Technical  
Memorandum No. 325. (Translation from German).

WATKINS, F. M., Hydraulic Loss in Pipe Bends, U.S.B.R. Technical Memo-  
randum No. 517.

WING, S. P., Appendix to Thoma's "Hydraulic Losses in Pipe Fittings,"  
U.S.B.R. Technical Memorandum No. 342.



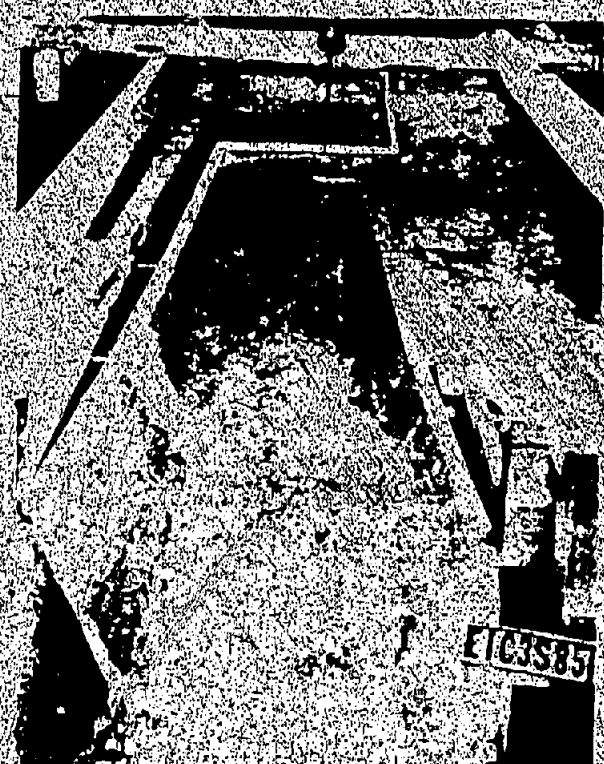
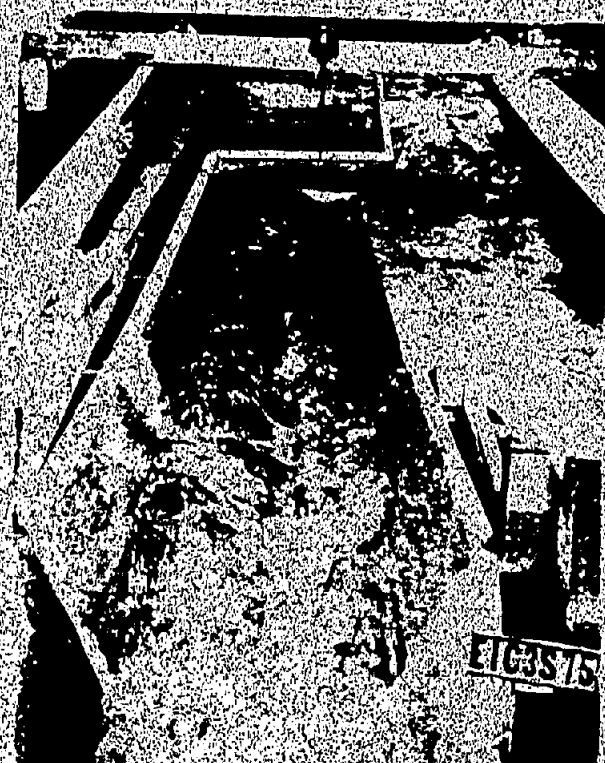


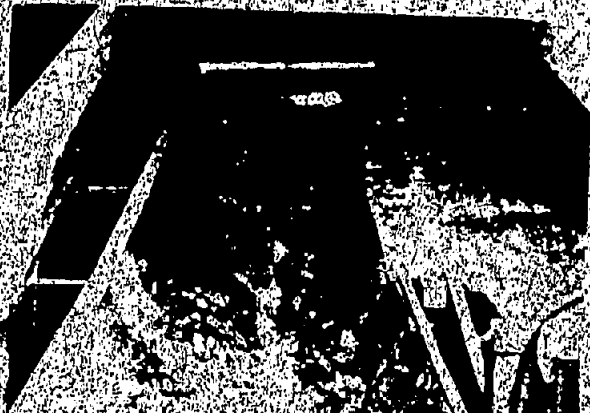
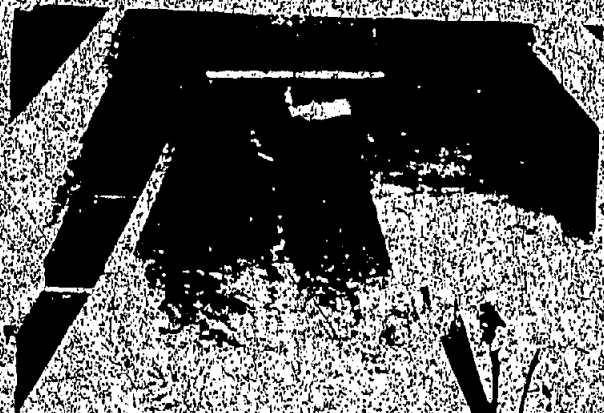
RED SAND - 2000 FT. DEEP  
DEPTH & CROSS-BELL ACTION - 2000 FT. DEEP





FIG. SANDY / DAU SPILL /  
CROSS-SECTION / SPILL QUANTITY No. 1





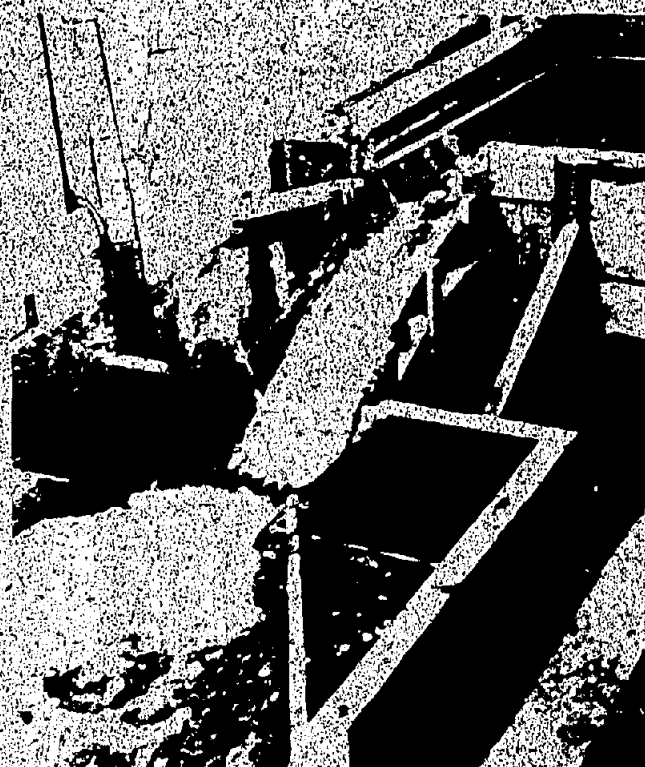
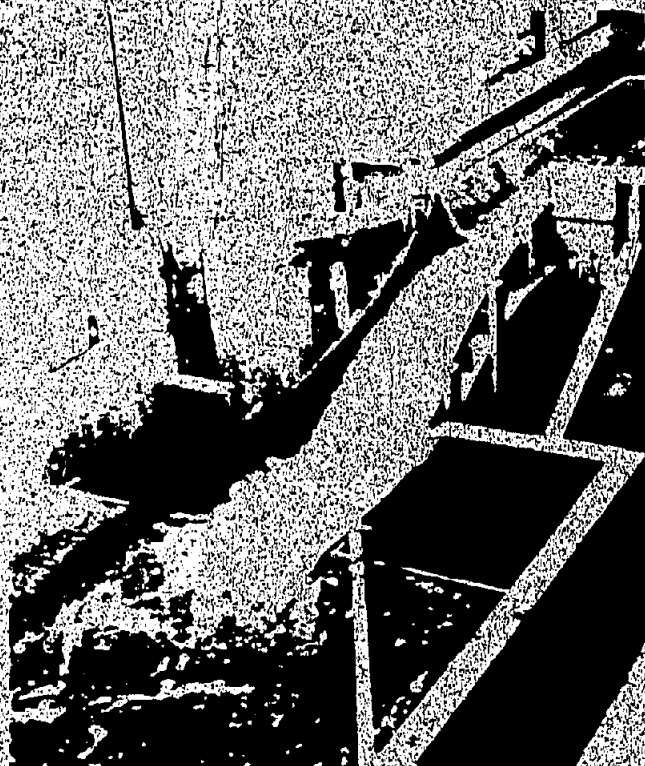
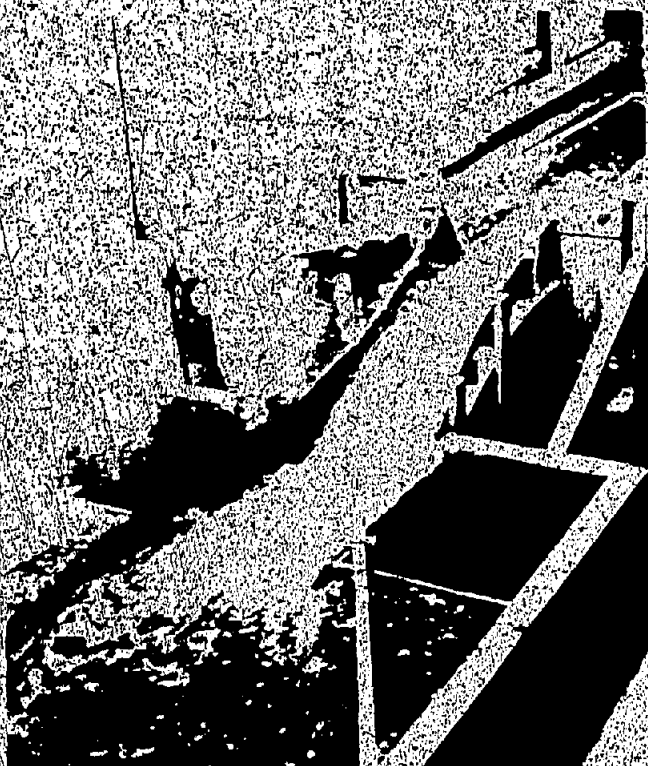
EIC3R75

EIC3R85



EIC3R120

EIC3R130



15. CONTAINER, AN AREA-  
CHANGING UNIT